

## Black-Hole Solution Without Curvature Singularity And Closed Timelike Curves

F.R. KLINKHAMER

Institute for Theoretical Physics, Karlsruhe Institute of Technology (KIT),  
76128 Karlsruhe, Germany

With a prescribed Coulomb-type energy-momentum tensor, an exact solution of the Einstein field equations over a nonsimply-connected manifold is presented. This spherically symmetric solution has neither curvature singularities nor closed timelike curves. It can be considered to be a regularization of the singular Reissner–Nordström solution over a simply-connected manifold.

PACS numbers: 04.20.Cv, 02.40.Pc, 04.20.Jb, 04.70.Dy

### 1. Introduction

The vacuum Einstein field equations over  $\mathcal{M}_4 = \mathbb{R}^4$  have a spherically symmetric solution, the Schwarzschild solution [1, 2, 3, 4]. Recently, a modification of the standard Schwarzschild solution has been suggested [5], which has no curvature singularity but does have closed timelike curves inside the Schwarzschild event horizon. Here, we show that a further modification allows us, in principle, to eliminate these closed timelike curves.

The basic idea is as follows. The problematic closed timelike curves of the modified Schwarzschild solution [5] trace back to the fact that the original singularity was *space-like* [4]. But it is well-known that the singularity of the standard Reissner–Nordström solution [6, 7, 8, 9] is *time-like*. This suggests, first, to add a small electric charge and, then, to modify the resulting Reissner–Nordström solution in order to arrive at a nonsingular black-hole solution without closed timelike curves.

## 2. Reissner–Nordström solution

In this article we use geometric units ( $G_N = c = 1$ ) and consider spherically symmetric solutions of the Einstein field equations [4],

$$R_{\mu}{}^{\nu} - \frac{1}{2} R \delta_{\mu}{}^{\nu} = 8\pi T_{\mu}{}^{\nu}, \quad (2.1a)$$

where the energy-momentum tensor  $T_{\mu}{}^{\nu}$  is set equal to a prescribed energy-momentum tensor  $\Theta_{\mu}{}^{\nu}$  (for spherical coordinates),

$$T_{\mu}{}^{\nu}(t, r, \theta, \phi) = \Theta_{\mu}{}^{\nu}(t, r, \theta, \phi) \equiv \frac{Q^2}{8\pi r^4} \left[ \text{diag}(-1, -1, 1, 1) \right]_{\mu}{}^{\nu}. \quad (2.1b)$$

This particular  $\Theta_{\mu}{}^{\nu}$  corresponds to the energy-momentum tensor of a Coulomb-type electric field.

The standard Reissner–Nordström (RN) solution [6, 7] has a metric in the exterior region given by the following line element:

$$ds^2 \Big|_{\text{RN}}^{r > r_+} = - \left( 1 - \frac{2M}{r} + \frac{Q^2}{r^2} \right) dt^2 + \left( 1 - \frac{2M}{r} + \frac{Q^2}{r^2} \right)^{-1} dr^2 + r^2 \left( d\theta^2 + \sin^2 \theta d\phi^2 \right), \quad (2.2)$$

with coordinates  $t \in \mathbb{R}$ ,  $r > r_+$ ,  $\theta \in [0, \pi]$ , and  $\phi \in [0, 2\pi)$ , where  $r_{\pm} \equiv M \pm \sqrt{M^2 - Q^2}$ . Here,  $M$  can be interpreted as the mass of the central object and  $Q$  as its electric charge.

The RN metric in the interior regions ( $r \leq r_+$ ) can best be described with other coordinates [4, 8, 9]. But, in the innermost region ( $r < r_-$ ), it is possible to revert to  $r$  and  $t$ , and the metric takes again the form (2.2).

## 3. Nonsingular black-hole solution with electric charge

### 3.1. Topology

The spacetime considered in this article corresponds to a noncompact, orientable, nonsimply-connected manifold  $\widetilde{\mathcal{M}}$  without boundary. This manifold has the topology

$$\widetilde{\mathcal{M}} = \mathbb{R} \times \widetilde{\mathcal{M}}_3, \quad (3.1a)$$

$$\widetilde{\mathcal{M}}_3 \simeq \mathbb{R}P^3 - \{\text{point}\}, \quad (3.1b)$$

where  $\mathbb{R}P^3$  is the 3-dimensional real projective space (topologically equivalent to a 3-sphere with antipodal points identified). The particular manifold

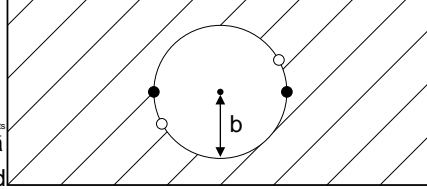


Figure 1. Three-space  $\widetilde{\mathcal{M}}_3$  obtained by surgery on  $\mathbb{R}^3$ : interior of the ball with radius  $b$  removed and antipodal points on the boundary of the ball identified (as indicated by open and filled circles).

$\widetilde{\mathcal{M}}_3$  has been discussed extensively in Refs. [10, 11, 12], but the present article aims to be self-contained and the necessary details will be provided.

The explicit construction of  $\widetilde{\mathcal{M}}_3$  is as follows: start from 3-dimensional Euclidean space  $E_3$ , remove the interior of a ball ( $r < b$ ), and identify antipodal points on the boundary ( $r = b$ ). See Fig. 1 for a sketch and App. A for details. The *Ansatz* metric will be given in terms of the time coordinate  $T \in \mathbb{R}$  and the proper coordinates of  $\widetilde{\mathcal{M}}_3$ . Note that the standard Cartesian coordinates of  $E_3$  are inappropriate: different Cartesian coordinates of  $E_3$  may correspond to a single point of  $\widetilde{\mathcal{M}}_3$  (an example is given by the filled circles in Fig. 1, which correspond to a unique point of  $\widetilde{\mathcal{M}}_3$ ).

The manifold  $\widetilde{\mathcal{M}}_3$  is covered by three coordinates charts,

$$(X_n, Y_n, Z_n), \quad (3.2)$$

for  $n = 1, 2, 3$ . These coordinates have the following ranges:

$$X_1 \in (-\infty, \infty), \quad Y_1 \in (0, \pi), \quad Z_1 \in (0, \pi), \quad (3.3a)$$

$$X_2 \in (0, \pi), \quad Y_2 \in (-\infty, \infty), \quad Z_2 \in (0, \pi), \quad (3.3b)$$

$$X_3 \in (0, \pi), \quad Y_3 \in (0, \pi), \quad Z_3 \in (-\infty, \infty). \quad (3.3c)$$

In each chart, there is one radial-type coordinate with infinite range, one polar-type angular coordinate of finite range, and one azimuthal-type angular coordinate of finite range. Further details can be found in App. B.

### 3.2. Parameters and solution

The nonsingular RN-type solution of the Einstein field equations has an additional parameter, the length  $b$  (an operational definition of  $b$  will be

given later). The three parameters of the solution are assumed to be related as follows:

$$0 < |Q| < M, \quad (3.4a)$$

$$0 < b < \zeta_-, \quad (3.4b)$$

with definitions

$$\zeta_{\pm} \equiv M \pm \sqrt{M^2 - Q^2}. \quad (3.5)$$

Note that, for the classical theory, the electric charge  $|Q|$  can be arbitrarily small, as long as it remains nonzero.

The construction of the nonsingular solution with parameters (3.4) involves an effective radial coordinate  $\zeta$ , defined in terms of the quasi-radial coordinates of  $\widetilde{\mathcal{M}}_3$  and the length parameter  $b$ . We refer to Carter's original article [9] for the conformal structure of the standard Reissner–Nordström solution and follow the same modification procedure as used in our previous article [5] for the Schwarzschild solution. As we are primarily interested in the removal of the curvature singularity, we focus on the spacetime region III ( $\zeta < \zeta_-$ ). No essential changes occur for the spacetime regions I and II ( $\zeta \geq \zeta_-$ ), because they do not reach the singularity (see Fig. 1b of Ref. [9] or Fig. 25 of Ref. [4]).

The construction starts with the chart-1 coordinates as presented in Sec. 3.1, the other two charts will be added afterwards. In terms of these chart-1 coordinates  $(T, X_1, Y_1, Z_1)$ , the *Ansatz* for the region–III line element is as follows:

$$\begin{aligned} ds^2 \Big|_{\text{chart-1}}^{b \leq \zeta < \zeta_-} &= - \left( 1 - \frac{2M}{\zeta} + \frac{Q^2}{\zeta^2} \right) dT^2 \\ &\quad + \left( 1 - \frac{2M}{\zeta} + \frac{Q^2}{\zeta^2} \right)^{-1} \frac{(X_1)^2}{\zeta^2} (dX_1)^2 \\ &\quad + \zeta^2 \left( (dZ_1)^2 + (\sin Z_1)^2 (dY_1)^2 \right), \end{aligned} \quad (3.6a)$$

$$\zeta \Big|_{\text{chart-1}} = \sqrt{b^2 + (X_1)^2}. \quad (3.6b)$$

As the apparent singularities at  $\zeta = \zeta_{\pm}$  in (3.6a) are away from the “stitched-up” surface at  $\zeta = b$  (referring to the surgery performed in App. A), the standard analysis [4, 9] in terms of  $T$  and  $\zeta$  coordinates shows that these apparent singularities can be removed by appropriate coordinate transformations.

This essentially completes the construction of our new metric (3.6). Note that (3.6a) takes precisely the form of the original Reissner–Nordström metric (2.2) if  $[(X_1)^2/\zeta^2] (dX_1)^2$  is replaced by  $d\zeta^2$  according to (3.6b). But, as emphasized in Ref. [5], the crucial point here is the appearance of the coordinate  $X_1 \in (-\infty, \infty)$  of the nonsimply-connected manifold  $\widetilde{\mathcal{M}}_3$ . In addition, there are now radial geodesics passing through  $X_1 = 0$ , as explained in Sec. 3 of Ref. [12].

The Riemann curvature tensor  $R^\kappa{}_{\lambda\mu\nu}(T, X_1, Y_1, Z_1)$  from the metric (3.6) is found to be even in  $X_1$  and finite at  $X_1 = 0$ . The Ricci tensor  $R_\mu{}^\nu(T, X_1, Y_1, Z_1)$  from (3.6) equals  $(Q^2/\zeta^4) \text{diag}(1, 1, -1, -1)$  and the Ricci scalar  $R(T, X_1, Y_1, Z_1)$  vanishes identically. The metric (3.6) solves, therefore, the Einstein field equations (2.1a) for a prescribed energy-momentum tensor  $\Theta_\mu{}^\nu(T, X_1, Y_1, Z_1)$  of the diagonal form (2.1b) with  $1/r^4$  replaced by  $1/\zeta^4 = 1/(b^2 + (X_1)^2)^2$ .

The results from App. B allow for an immediate extension of the metric (3.6) of the  $n = 1$  chart to the metrics of the  $n = 2$  and  $n = 3$  charts:

$$ds^2 \Big|_{\text{chart-2}}^{b \leq \zeta < \zeta^-} = - \left( 1 - \frac{2M}{\zeta} + \frac{Q^2}{\zeta^2} \right) dT^2 + \left( 1 - \frac{2M}{\zeta} + \frac{Q^2}{\zeta^2} \right)^{-1} \frac{(Y_2)^2}{\zeta^2} (dY_2)^2 + \zeta^2 \left( (dZ_2)^2 + (\sin Z_2)^2 (dX_2)^2 \right), \quad (3.7a)$$

$$\zeta \Big|_{\text{chart-2}} = \sqrt{b^2 + (Y_2)^2}, \quad (3.7b)$$

and

$$ds^2 \Big|_{\text{chart-3}}^{b \leq \zeta < \zeta^-} = - \left( 1 - \frac{2M}{\zeta} + \frac{Q^2}{\zeta^2} \right) dT^2 + \left( 1 - \frac{2M}{\zeta} + \frac{Q^2}{\zeta^2} \right)^{-1} \frac{(Z_3)^2}{\zeta^2} (dZ_3)^2 + \zeta^2 \left( (dY_3)^2 + (\sin Y_3)^2 (dX_3)^2 \right), \quad (3.8a)$$

$$\zeta \Big|_{\text{chart-3}} = \sqrt{b^2 + (Z_3)^2}. \quad (3.8b)$$

The corresponding Kretschmann curvature scalar over the different charts is given by

$$K \equiv R_{\mu\nu\rho\sigma} R^{\mu\nu\rho\sigma} = \frac{8(6M^2\zeta^2 - 12MQ^2\zeta + 7Q^4)}{\zeta^8}, \quad (3.9)$$

which remains finite because  $\zeta > 0$  for  $b > 0$ . With fixed values of  $M$  and  $Q$  obeying condition (3.4a),  $K(\zeta)$  drops monotonically with  $\zeta$ . This fact allows for an operational definition of  $b$  from the maximum value of  $K$ . (The operational definitions of  $M$  and  $Q$  rely, for example, on the asymptotic  $\zeta \rightarrow \infty$  behavior of the metric and electromagnetic field.) Note that the actual value of  $b$  sets the length of the shortest possible noncontractible loop in the spacelike hypersurface with constant  $T$  (such a loop corresponds to half of a great circle on the sphere  $\zeta = b$ , taken between antipodal points which are identified).

The spacetime with metrics (3.6)–(3.8) corresponds to a noncompact, orientable, nonsimply-connected manifold without boundary and has the topology (3.1). The main result of this article is that the factor  $\mathbb{R}$  in (3.1a) corresponds to the timelike direction of the metrics (3.6)–(3.8), making for a spacelike hypersurface  $\widetilde{\mathcal{M}}_3$  in the spacetime region III. In turn, this observation implies the absence of closed timelike curves.<sup>1</sup>

#### 4. Discussion

The nonsingular solution (3.6)–(3.8) with parameters (3.4) provides a “regularization” of the singular Reissner–Nordström solution. But this regularized spacetime does have a “blemish,” as mentioned in the Note Added of Ref. [5] and detailed in Appendix D of Ref. [12]. The fact is that the coordinate transformation which brings the manifold (3.6) near  $X_1 = 0$  to a patch of Minkowski spacetime is a  $C^1$  function with a discontinuous second derivative at  $X_1 = 0$  (that is, not a genuine diffeomorphism, which is a  $C^\infty$  function everywhere). Whether or not such a classical spacetime without the standard elementary-flatness property (having a type of “spacetime defect”) plays a role in physics may be up to quantum gravity to decide, at least according the following scenario [5].

Start from a nearly flat spacetime (trivial topology  $\mathbb{R}^4$  and metric approximately equal to the Minkowski metric), where a large amount of matter with total mass  $M$  and with vanishing net charge  $Q = 0$  is arranged to collapse in a spherically symmetric way. Within the realm of classical Einstein gravity, we expect to end up with the singular Schwarzschild solution.

But, very close to the final curvature singularity, something else may happen due to quantum effects. Considering a precursor mass  $\Delta M \sim \hbar/(bc) \ll M$  and using typical curvature values from the expressions for the Kretschmann scalar, the local spacetime integral of the action density related to the Schwarzschild solution differs from that related to (3.6) by an amount  $\lesssim \hbar$ . Then, as argued by Wheeler in particular, the local topology

---

<sup>1</sup> Note that the spacetime regions I ( $\zeta > \zeta_+$ ) and II ( $\zeta_- < \zeta < \zeta_+$ ) do not reach the  $\zeta = b$  surface where antipodal points are identified (*cf.* Fig. 1).

of the manifold may change by a quantum jump if  $b$  is sufficiently close to  $L_{\text{Planck}} \equiv (\hbar G_N/c^3)^{1/2}$ . In addition, the strong gravitational fields may lead to electron-positron pair creation, possibly with one charge expelled towards spatial infinity.

These two quantum processes combined may result in a transition from a simply-connected manifold without localized charge to a nonsimply-connected manifold with localized charge  $Q = \pm |Q_{\text{electron}}| \equiv \pm e$ . Hence, if the transition amplitude between the different topologies is nonzero for appropriate matter content, quantum mechanics can operate a change between the classical Schwarzschild solution and the classical solution (3.6) with  $Q = \pm e$  and an additional charge  $\mp e$  at infinity, thereby removing the curvature singularity while avoiding closed timelike curves. The removal of the curvature singularity comes at the price of introducing a type of spacetime defect (the blemish mentioned above). The underlying quantum theory of gravity must determine if such spacetime defects are allowed or not.

### Acknowledgments

This work has been supported, in part, by the ‘‘Helmholtz Alliance for Astroparticle Physics (HAP),’’ funded by the Initiative and Networking Fund of the Helmholtz Association.

### Appendix A

#### *Manifold*

The explicit construction of the 3-space  $\widetilde{M}_3$  proceeds by local surgery [10] on the 3-dimensional Euclidean space  $E_3 = (\mathbb{R}^3, \delta_{mn})$ . It is convenient to use standard Cartesian and spherical coordinates,

$$\vec{x} = (x^1, x^2, x^3) = (r \sin \theta \cos \phi, r \sin \theta \sin \phi, r \cos \theta), \quad (\text{A.1})$$

with  $x^m \in (-\infty, +\infty)$ ,  $r \geq 0$ ,  $\theta \in [0, \pi]$ , and  $\phi \in [0, 2\pi)$ .

Now,  $\widetilde{M}_3$  is obtained from  $\mathbb{R}^3$  by removal of the interior of the ball  $B_b$  with radius  $b$  and identification of antipodal points on the boundary  $S_b \equiv \partial B_b$ . With point reflection denoted  $P(\vec{x}) = -\vec{x}$ , the 3-space  $\widetilde{M}_3$  is given by

$$\widetilde{M}_3 = \left\{ \vec{x} \in \mathbb{R}^3 : (|\vec{x}| \geq b > 0) \wedge (P(\vec{x}) \cong \vec{x} \text{ for } |\vec{x}| = b) \right\}, \quad (\text{A.2})$$

where  $\cong$  stands for point-wise identification (Fig. 1).

It can be shown that  $\widetilde{M}_3$  is a manifold [10, 11] and appropriate coordinate charts will be given in App. B. Preparing for that discussion, introduce already the following nonstandard spherical coordinates  $(r, \vartheta, \varphi)$  on  $\mathbb{R}^3$ :

$$(x^1, x^2, x^3) = (r \sin \vartheta \sin \varphi, r \cos \vartheta, r \sin \vartheta \cos \varphi), \quad (\text{A.3})$$

with  $r \geq 0$ ,  $\vartheta \in [0, \pi]$ , and  $\varphi \in [0, 2\pi)$ .

## Appendix B

### Coordinate charts

The 3-space  $\widetilde{M}_3$  was defined in App. A and shown in Fig. 1. A relatively simple covering [11] of  $\widetilde{M}_3$  uses three charts of coordinates, labeled by  $n = 1, 2, 3$ . Each chart covers and surrounds part of one of the three Cartesian coordinate axes but does not intersect the other two Cartesian coordinate axes. For example, the  $n = 1$  coordinate chart covers and surrounds the  $|x^1| \geq b$  segments of the  $x^1$  coordinate axis but does not intersect the  $x^2$  and  $x^3$  axes. The domains of the chart-1 coordinates consist of two ‘wedges,’ on both sides of the defect and pierced by the  $x^1$  axis; see Fig. 2.

These coordinates are denoted  $(X_n, Y_n, Z_n)$ , for  $n = 1, 2, 3$ . Note that, despite appearances, the triples  $(X_n, Y_n, Z_n)$  are non-Cartesian coordinates.

Referring to the standard spherical coordinates (A.1) of the Euclidean 3-space  $E_3$ , the chart-1 coordinates over the relevant regions of  $\widetilde{M}_3$  (*i.e.*, the

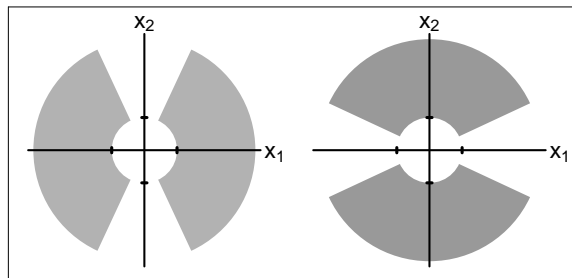


Figure 2. Slice  $x_3 = 0$  of the manifold  $\widetilde{M}_3$  with the domains of the chart-1 coordinates (left) and the chart-2 coordinates (right). The tick marks on the  $x_1$  and  $x_2$  axes correspond to the values  $\pm b$  (see Fig. 1). The 3-dimensional domains are obtained by revolution around the  $x_1$ -axis (left) or the  $x_2$ -axis (right). The domain of the chart-3 coordinates is defined similarly.

wedges of Fig. 2, left) are given by

$$X_1 = \begin{cases} r - b & \text{for } \cos \phi > 0, \\ b - r & \text{for } \cos \phi < 0, \end{cases} \quad (\text{B.1a})$$

$$Y_1 = \begin{cases} \phi - \pi/2 & \text{for } \pi/2 < \phi < 3\pi/2, \\ \phi - 3\pi/2 & \text{for } 3\pi/2 < \phi < 2\pi, \\ \phi + \pi/2 & \text{for } 0 \leq \phi < \pi/2, \end{cases} \quad (\text{B.1b})$$

$$Z_1 = \begin{cases} \theta & \text{for } \cos \phi > 0, \\ \pi - \theta & \text{for } \cos \phi < 0, \end{cases} \quad (\text{B.1c})$$

with ranges

$$X_1 \in (-\infty, \infty), \quad Y_1 \in (0, \pi), \quad Z_1 \in (0, \pi). \quad (\text{B.1d})$$

The construction of the chart-2 coordinates is entirely analogous to those of the chart  $n = 1$ . Specifically, this set of coordinates over the relevant regions (wedges of Fig. 2, right) of  $\widetilde{M}_3$  is given by

$$X_2 = \begin{cases} \phi & \text{for } 0 < \phi < \pi, \\ \phi - \pi & \text{for } \pi < \phi < 2\pi, \end{cases} \quad (\text{B.2a})$$

$$Y_2 = \begin{cases} r - b & \text{for } 0 < \phi < \pi, \\ b - r & \text{for } \pi < \phi < 2\pi, \end{cases} \quad (\text{B.2b})$$

$$Z_2 = \begin{cases} \theta & \text{for } 0 < \phi < \pi, \\ \pi - \theta & \text{for } \pi < \phi < 2\pi. \end{cases} \quad (\text{B.2c})$$

with ranges

$$X_2 \in (0, \pi), \quad Y_2 \in (-\infty, \infty), \quad Z_2 \in (0, \pi). \quad (\text{B.2d})$$

For the  $n = 3$  chart, we require nonstandard spherical coordinates that are regular on the Cartesian  $x^3$  axis. These have been defined in (A.3). Now, the chart-3 coordinates over the relevant regions (wedges) of  $\widetilde{M}_3$  are given by

$$X_3 = \begin{cases} \varphi - \pi/2 & \text{for } \pi/2 < \varphi < 3\pi/2, \\ \varphi - 3\pi/2 & \text{for } 3\pi/2 < \varphi < 2\pi, \\ \varphi + \pi/2 & \text{for } 0 \leq \varphi < \pi/2, \end{cases} \quad (\text{B.3a})$$

$$Y_3 = \begin{cases} \vartheta & \text{for } \cos \varphi > 0, \\ \pi - \vartheta & \text{for } \cos \varphi < 0, \end{cases} \quad (\text{B.3b})$$

$$Z_3 = \begin{cases} r - b & \text{for } \cos \varphi > 0, \\ b - r & \text{for } \cos \varphi < 0, \end{cases} \quad (\text{B.3c})$$

with ranges

$$X_3 \in (0, \pi), \quad Y_3 \in (0, \pi), \quad Z_3 \in (-\infty, \infty). \quad (\text{B.3d})$$

Having expressed the coordinates  $(X_n, Y_n, Z_n)$  in terms of coordinates of the Euclidean 3-space, it is possible to verify that the  $(X_n, Y_n, Z_n)$  coordinates are invertible and infinitely-differentiable functions of each other in the overlap regions. These coordinates therefore describe a manifold. Moreover, the manifold satisfies [11] the Hausdorff property (two distinct points  $x$  and  $y$  are always surrounded by two disjoint open sets  $U$  and  $V$ :  $x \in U$ ,  $y \in V$ , and  $U \cap V = \emptyset$ ).

### References

- [1] K. Schwarzschild, "Über das Gravitationsfeld eines Massenpunktes nach der Einsteinschen Theorie," *Sitzungsberichte der Deutschen Akademie der Wissenschaften zu Berlin, Klasse für Mathematik, Physik, und Technik*, pp. 189–196 (1916).
- [2] M.D. Kruskal, "Maximal extension of Schwarzschild metric," *Phys. Rev.* **119**, 1743 (1960).
- [3] G. Szekeres, "On the singularities of a Riemannian manifold," *Publ. Math. Debrecen* **7**, 285 (1960).
- [4] S.W. Hawking and G.F.R. Ellis, *The Large Scale Structure of Space-Time*, Cambridge Univ. Press, Cambridge, England, 1973.
- [5] F.R. Klinkhamer, "Black-hole solution without curvature singularity," *Mod. Phys. Lett. A* **28**, 1350136 (2013), arXiv:1304.2305.
- [6] H. Reissner, "Über die Eigengravitation des elektrischen Feldes nach der Einsteinschen Theorie," *Annalen der Physik* **50**, 106 (1916).
- [7] G. Nordström, "On the energy of the gravitational field in Einstein's theory," *Proceedings Academy of Sciences of Amsterdam* **26**, 1201 (1918).
- [8] J.C. Graves and D.R. Brill, "Oscillatory character of Reissner-Nordstrom metric for an ideal charged wormhole," *Phys. Rev.* **120**, 1507 (1960).
- [9] B. Carter, "The complete analytic extension of the Reissner-Nordström metric in the special case  $e^2 = m^2$ ," *Phys. Lett.* **21**, 423 (1966).
- [10] S. Bernadotte and F.R. Klinkhamer, "Bounds on length scales of classical spacetime foam models," *Phys. Rev. D* **75**, 024028 (2007), arXiv:hep-ph/0610216.
- [11] M. Schwarz, *Nontrivial Spacetime Topology, Modified Dispersion Relations, and an  $SO(3)$ -Skyrme Model* (PhD Thesis, KIT, July 2010), Verlag Dr. Hut, München, Germany, 2010.
- [12] F.R. Klinkhamer, "A new type of nonsingular black-hole solution in general relativity," arXiv:1309.7011.